Progress In Electromagnetics Research B, Vol. 41, 333–356, 2012

MARGINAL MOMENT GENERATING FUNCTION BASED ANALYSIS OF CHANNEL CAPACITY OVER CORRELATED NAKAGAMI-m FADING WITH MAXIMAL-RATIO COMBINING DIVERSITY

V. K. Dwivedi[1] and G. Singh[2, *]

[1]Department of Electronics and Communication Engineering, Jaypee Institute of Information Technology, Noida 230123, India

[2]Department of Electronics and Communication Engineering, Jaypee University of Information Technology, Waknaghat, Solan 173234, India

Abstract—In this paper, we have investigated the marginal moment generating function (MMGF) for the correlated Nakagami-m fading channel by using maximal-ratio combining (MRC) diversity scheme at receiver for the computation of channel capacity for various adaptive transmission schemes such as: 1) optimal simultaneous power and rate adaptation, 2) optimal rate adaptation with constant transmit power, 3) channel inversion with fixed rate, and 4) truncated channel inversion with fixed rate. The effects of diversity receiver as well as correlation coefficients on all these transmission schemes are discussed and the channel capacity obtained using this proposed approach for all schemes is compared with reported literature.

1. INTRODUCTION

Recently, the demand of wireless communication is growing explosively, therefore it is very important to determine the capacity limits of fading channels. In general, the capacity in fading channel is a complex expression in terms of the channel variation in time and/or frequency depending upon the transmitter and/or receiver knowledge of the channel side information [1–4]. Earlier, the channel capacity has been studied by various researchers for several fading environments [5–16]. In [5], Goldsmith and Varaiya have examined the capacity of Rayleigh fading channels under different adaptive transmission techniques. In [6], Lee has derived an expression for the channel capacity for

Received 19 April 2012, Accepted 11 June 2012, Scheduled 16 June 2012
* Corresponding author: Ghanshyam Singh (drghanshyam.singh@yahoo.com).

Rayleigh fading channel. In [7], Gunther has extended the results presented in [6] by deriving the capacity of Rayleigh fading channels under diversity scheme. In [8], Alouini and Goldsmith have derived the capacity of Rayleigh fading channels under different diversities as well as rate adaptation and transmit power schemes. Other fading channels like Nakagami, Weibull, Rician, and Hoyt fading channels were studied in [9, 10]. In [11], Khatalin and Fonseka have discussed the channel capacity for correlated Nakagami-m fading channel using dual-diversity. In [12], the channel capacity under different diversity schemes and different rate adaptation and transmit power schemes for the correlated Rayleigh fading channel have been derived. In [13], the characteristics function (CF) is developed for computing the ergodic channel capacity. In [14, 15], the moment generating function based (MGF) approach is proposed for the computation of channel capacity with optimal rate adaptation (C_{ORA}) scheme only by using numerical techniques. In [16], a novel MGF based approach is developed for evaluation of the channel capacity for various rate adaptations and transmit power schemes. In [16], the integral is evaluated by using mainly two types of numerical technique and both the numerical techniques are lengthy and much more complex. In [17], the channel capacity limitation for the fading channel is discussed.

In this paper, we have presented a marginal moment generating function (MMGF) based channel capacity analysis over correlated Nakagami-m fading channel with M-branch MRC diversity. The main contribution of this paper consists of the evaluation of MMGF function and the derived MMGF function is used to obtain a closed-form mathematical expression for the channel capacity with optimal rate and power adaptation (C_{OPRA}), Truncated CIFR (C_{TCIFR}) approach and MGF is used to derive expression of the channel inversion with fixed rate (C_{CIFR}), channel capacity under optimal rate adaptation (C_{ORA}) because MGF is a special case of MMGF by using lower limit equal to zero then MMGF is converted into MGF as shown in next section. The derived expressions are in terms of well known Meijer G function and other special functions, which can be easily implemented by using Maple or Mathematica software. The remainder of the paper is organized as follows. Section 2 describes the system model. In Section 3, MMGF is evaluated. The channel capacity evaluation under different policies is performed in the Section 4. Numerical results are discussed in the Section 5. Finally, the Section 6 concludes the work.

2. CHANNEL MODEL

Consider an M-branch maximal ratio combing (MRC) diversity receiver. The received base-band signal on ith branch can be written as:

$$r_i(t) = s(t)\, H_i e^{j\phi_k} + n_i(t), \qquad i = 1, 2, \ldots, M \tag{1}$$

where $s(t)$ is the transmitted signal and $n_k(t)$ is the identically distributed white Gaussian noise with zero-mean. ϕ_k is the uniformly distributed over range $[0,\ 2\pi)$ and H_i is the Nakagami-m distributed signal envelop with a probability distribution function as given in [1]

$$f_{H_i}(H_i) = \frac{2}{\Gamma(m_k)} \cdot \left(\frac{m_i}{\Omega_i}\right)^{m_i} \cdot H_i^{2m_i - 1} \cdot e^{-(m_i/\Omega_i)H_i^2} \qquad i = 1, 2, \ldots, M \tag{2}$$

where $\Gamma(\cdot)$ is the Gamma function and $\Omega_i = \bar{H}_i^2$ is the average power on kth branch. $m_i \geq 1/2$ is the fading parameter, which is discussed in detail in [1]. $m_i = 1$ and $m_i = \infty$ corresponds to the Rayleigh and non-fading channel [1], respectively. The smaller value of the m_i represents the more fading in the channel. We have also considered that the average power of signal (Ω_i) as well as the fading parameters (m_i) in each M-channel MRC diversity system, which is identical. The assumption of identical power is reasonable if the diversity channels are closely spaced and the gain of each channel is such that all the noise power is same in each [18]. The instantaneous signal-to-noise ratio (SNR) at output of MRC diversity is given by [18–20]:

$$\gamma_t = \frac{E_S}{N_\circ} \sum_{i=1}^{M} |H_i|^2 = \sum_{i=1}^{M} \gamma_i \tag{3}$$

where E_S is the average symbol energy, and N_0 is the single sided power spectral density of the Gaussian noise. When the receiving antennas are closely spaced then receiving signals are also correlated, hence the SNR of received signals $\gamma_{1,}\gamma_2 \ldots \gamma_{\mathrm{M}}$ cannot be considered as independent random variables. The correlation coefficient between two receiving antenna is (by assuming equal correlation between antennas ρ) given as [1]:

$$\rho = Cov(\gamma_i, \gamma_j) \Big/ \sqrt{Var(\gamma_i)\, Var(\gamma_j)} \quad 0 \leq \rho < 1 \tag{4}$$

where $j = 1 \ldots M$. $Cov(\gamma_i, \gamma_j)$ is the covariance of γ_i and γ_j. $Var(\cdot)$ is the variance. The probability density function of γ_t for the correlated

Nakagami fading is given as [21]:

$$f_\gamma(\gamma_t) = \frac{\left(\frac{\gamma_t\, m}{\bar{\gamma}_t}\right)^{M m-1} \exp\left(\frac{-\gamma_t m}{\bar{\gamma}_t\ (1-\rho)}\right)\ {}_1F_1\left(m, Mm, \frac{M\, m\, \rho\, \gamma_t}{\bar{\gamma}_t(1-\rho)(1-\rho+M\rho)}\right)}{\left(\frac{\bar{\gamma}_t}{m}\right)(1-\rho)^{m(M-1)}\ (1-\rho+M\rho)^m\, \Gamma(M\, m)}$$

$$\gamma_t > 0 \qquad (5)$$

where $\bar{\gamma}_t$ is average SNR, and ${}_1F_1(\cdot)$ is the confluent hyper geometric function as given in [22, 23]. On the other hand, recent advances on performance analysis of the digital communication systems in fading channel has recognized the potential importance of the moment generating function (MGF) as a powerful tool for simplifying the analysis of diversity communication systems. This has led to simple expressions for average bit-error-rate and symbol-error-rate in variety of digital signalling schemes in the fading channels, including multichannel reception with correlated diversity. If we consider: $A = \left(\frac{m}{\bar{\gamma}_t}\right)^{Mm}$, $B = \frac{m}{\bar{\gamma}_t(1-\rho)}$, $C = \frac{M\, m\, \rho}{\bar{\gamma}_t(1-\rho)(1-\rho+M\rho)}$ and $D = (1-\rho)^{m(M-1)}\ (1-\rho+M\rho)^m\, \Gamma(M\, m)$.

Then Equation (5) can be written as:

$$f_\gamma(\gamma_t) = \frac{A}{D}\ e^{-B\,\gamma_t}{}_1F_1\left(m, Mm, C\gamma_t\right)(\gamma_t)^{Mm-1} \qquad (6)$$

3. MARGINAL MOMENT GENERATING FUNCTION EVALUATION

In this section, the MMGF of the SNR of M-branch MRC diversity is evaluated and further it is used to obtain the channel capacity. The MMGF is defined as [24]:

$$\hat{M}(s,a) = \int_a^\infty e^{-s\gamma} f_\gamma(\gamma) d\gamma \qquad (7)$$

By substituting the value of $f_\gamma(\gamma_t)$ from the Equation (6), we get:

$$\hat{M}(s,\gamma_0) = \frac{A}{D}\int_{\gamma_\circ}^\infty (\gamma_t)^{Mm-1} e^{-B\,\gamma_t}{}_1F_1\left(m, Mm, C\gamma_t\right) e^{-s\gamma_t} d\gamma_t \qquad (8)$$

By expanding ${}_1F_1(\cdot)$ from [22 Equation (9.14.1)] and putting in the Equation (8), we get:

$$\hat{M}(s,a) = \frac{A}{D}\sum_{k=0}^\infty \frac{\Gamma(k+m)\Gamma(Mm)}{\Gamma(m)\Gamma(k+Mm)}\frac{(C)^k}{k!} I_1 \qquad (9)$$

where

$$I_1 = \int_{\gamma_\circ}^{\infty} (\gamma_t)^{k+Mm-1} e^{-(s+B)\gamma_t} d\gamma_t \tag{10}$$

From [22 Equation (3.381.3)], the Equation (10) can be written as:

$$I_1 = (B+s)^{-(k+mM)}\,\Gamma(k+mM, a\,(B+s)) \tag{11}$$

By putting the result of I_1 from the Equation (11) into Equation (9), we get:

$$\hat{M}(s,a) = \frac{A}{D}\sum_{k=0}^{\infty} \frac{\Gamma(k+m)\Gamma(Mm)}{\Gamma(m)\Gamma(k+Mm)} \frac{(C)^k}{k!} \frac{\Gamma(k+mM, a\,(B+s))}{(B+s)^{(k+mM)}} \tag{12}$$

By putting $a = 0$ in Equation (12), the MMGF changs to MGF:

$$\begin{aligned} M(s) &= \frac{A}{D} \sum_{k=0}^{\infty} \frac{\Gamma(k+m)\Gamma(Mm)}{\Gamma(m)\Gamma(k+Mm)} \frac{(C)^k}{k!} \frac{\Gamma(k+mM,0)}{(B+s)^{(k+mM)}} \\ &= \frac{A}{D}\Gamma(Mm) \sum_{k=0}^{\infty} \frac{\Gamma(k+m)}{\Gamma(m)\ (B+s)^{(mM)}} \frac{1}{k!} \left(\frac{C}{B+s}\right)^k \\ M(s) &= \frac{A}{D}\Gamma(Mm) \times \sum_{k=0}^{\infty} \frac{\Gamma(k+m)}{\Gamma(m)} \frac{1}{k!}\ (C)^k \frac{1}{(B+s)^{Mm+k}} \end{aligned} \tag{13}$$

By using [22 Equation (9.140.1)], Equation (13) can be expressed as:

$$M(s) = \frac{A}{D} \frac{\Gamma(Mm)}{(B+s)^{Mm}} \times {}_2F_1\left(m, Mm; Mm; \frac{C}{B+s}\right) \tag{14}$$

where ${}_2F_1(\cdot)$ is the Gauss hypergeometric function [25]. By using [25 Equation (15.1.8)], Equation (14) can also be expressed as:

$$M(s) = \left(1 + \frac{\bar{\gamma}_t(1-\rho+M\rho)\,s}{m}\right)^{-m} \left(1 + \frac{\bar{\gamma}_t(1-\rho)\,s}{m}\right)^{-m(M-1)} \tag{15}$$

MGF in Equation (15) is further used to obtain the channel capacity under various adaptive schemes.

4. MARGINAL MGF BASED CHANNEL CAPACITY ANALYSIS

The channel capacity has been regarded as the fundamental information theoretic performance measure to predict the maximum information rate of a communication system. It is extensively used as the basic tool for the analysis and design of new and more efficient techniques to improve the spectral efficiency of modern wireless communication systems and to gain insight into how to counteract the detrimental effects of the multipath fading propagation via opportunistic and adaptive communication methods. The main reason for the analysis of the spectral efficiency over fading channels is represented by the fact that most framework described in various literature make use of the so-called PDF based approach of the received SNR has to be used, which is a task that might be very cumbersome for most system setups and often require to manage expression including series. It is also well known that a prior knowledge of channel state information at the transmitter may be exploited to improve the channel capacity, such that in the low SNR regime, the maximum achievable data rate of a fading channel might be much larger than that of without fading.

4.1. Optimal Rate Adaptation

When the transmitter power remains constant and channel state information (CSI) being available at the receiver side only. The channel capacity with optimal rate adaptation (C_{ORA}) in terms of the MGF based approach can be expressed as [18]:

$$C_{\mathrm{ORA}} = \frac{1}{\ln(2)} \int_0^\infty E_i(-s)\ M_\gamma^{(1)}(s)\, ds \tag{16}$$

where $E_i\left(\cdot\right)$ denotes the exponential integral function as defined in [23,] and $M_\gamma^{(1)}(s)$ is the first derivative of the MGF. The integral in Equation (16) is called as E_i-transform. Moreover, in those scenarios where very complicated expressions of MGF of the received SNR do not allow computing easily the aforementioned integral in a closed-form, the result in Equation (16) can be numerically evaluated by using standard software such as Maple and Mathematica [18]. Here, we have presented a closed-form expression for C_{ORA} scheme. By differentiating, Equation (12) with respect to s, we get:

$$M^1(s) = -\frac{A}{D}\Gamma(Mm) \times \sum_{k=0}^{\infty} \frac{\Gamma(k+m)}{\Gamma(m)} \frac{1}{k!}\ (c)^k\ \frac{(Mm+k)}{(B+s)^{Mm+k+1}} \tag{17}$$

By putting the value of $M^1(s)$ in Equation (16), we get,

$$C_{\mathrm{ORA}} = -\frac{1}{\ln(2)}\frac{A}{D}\Gamma(Mm) \times \sum_{k=0}^{\infty} \frac{\Gamma(k+m)}{\Gamma(m)} \frac{(Mm+k)}{k!}\ (c)^k\, I_2 \tag{18}$$

where

$$I_2 = \int_0^\infty E_i(-s)\,\frac{1}{(B+s)^{Mm+k+1}}ds$$
$$= \frac{1}{(B)^{Mm+k+1}}\int_0^\infty E_i(-s)\,\frac{1}{\left(1+\frac{s}{B}\right)^{Mm+k+1}}ds \tag{19}$$

By putting $\frac{s}{B} = t$ in Equation (19), and after some mathematical manipulations, we get:

$$I_2 = \frac{1}{(B)^{Mm+k}}\int_0^\infty \frac{E_i(-Bt)}{(1+t)^{Mm+k+1}}\,dt \tag{20}$$

From [23 Equation (8.4.2.7)] along with [23 Equation (8.4.11.1)], the Equation (20) can be expressed as:

$$I_2 = -\frac{1}{(B)^{Mm+k}\Gamma(k+mM+1)}\int_0^\infty G\begin{smallmatrix}1 & 1\\ 1 & 1\end{smallmatrix}\left[t\,\middle|\,\begin{matrix}-(k+Mm)\\ 0\end{matrix}\right] G\begin{smallmatrix}2 & 0\\ 1 & 2\end{smallmatrix}\left[Bt\,\middle|\,\begin{matrix}1 & \\ 0 & 0\end{matrix}\right]dt \tag{21}$$

By using [23 Equation (2.24.1)], the Equation (19) can be expressed as:

$$I_2 = \frac{G\begin{smallmatrix}3 & 1\\ 2 & 3\end{smallmatrix}\left[B\,\middle|\,\begin{matrix}0 & & 1\\ 0 & 0 & (k+mM)\end{matrix}\right]}{(B)^{Mm+k}\Gamma(k+mM+1)} \tag{22}$$

By putting value of I_2 from Equation (22) to the Equation (18), we get:

$$C_{\mathrm{ORA}} = \frac{1}{\ln(2)}\frac{A}{D}\Gamma(Mm)\times\sum_{k=0}^{\infty}\frac{\Gamma(k+m)}{\Gamma(m)}\frac{(Mm+k)}{k!}(C)^k$$
$$\frac{G\begin{smallmatrix}3 & 1\\ 2 & 3\end{smallmatrix}\left[B\,\middle|\,\begin{matrix}0 & & 1\\ 0 & 0 & (k+mM)\end{matrix}\right]}{(B)^{Mm+k}\Gamma(k+mM+1)} \tag{23}$$

where $G(\bullet)$ is Meijer's G function [22, Equation (9.301)]. An expression of C_{ORA} in Equation (23) shows the summation of infinite series but it diverges rapidly with the increasing the number of terms and only six terms are required to get closed form expression of C_{ORA}.

4.2. Optimal Simultaneous Power and Rate Adaptation

When both the transmitter and receiver have perfect channel information, then the channel capacity for the optimal power and rate adaptation (C_{OPRA}) is given by [8]:

$$C_{\mathrm{OPRA}} = B \int_{\gamma_\circ}^{\infty} \log_2\left(\frac{\gamma}{\gamma_\circ}\right) f_\gamma(\gamma)\, d\gamma \tag{24}$$

where B is the channel bandwidth (in Hz), and $\gamma_\circ$ is the optimal cut-off SNR level below which no transmission takes place. This optimal cut-off SNR level must satisfy:

$$\int_{\gamma_\circ}^{\infty} \left(\frac{1}{\gamma_\circ} - \frac{1}{\gamma}\right) f_\gamma(\gamma)\, d\gamma = 1 \tag{25}$$

to achieve the significant channel capacity, the amount of fading must be tracked at both the transmitter and receiver, the transmitter adapts its power and data rate to the channel variations by allocating high-power levels and rates for good channel condition and low power levels and rates for bad channel condition [8]. Furthermore, this optimal policy suffers a probability of outage P_{out}, which is equal to the probability of no transmission, as given by:

$$P_{\mathrm{out}} = \int_0^{\gamma_\circ} f_\gamma(\gamma)\, d\gamma \tag{26}$$

Now, an alternate method to evaluate the C_{OPRA} by using the MMGF is as given below. By substituting first $\gamma = q + \gamma_\circ$ in the Equation (24) and then again substituting $q/\gamma_\circ = x$ in the Equation (22). The Equation (23) is reduces to:

$$\begin{aligned} C_{\mathrm{OPRA}} &= \frac{\gamma_0}{\ln(2)} \int_0^{\infty} \ln(1+x)\, f_\gamma(\gamma_\circ(1+x))\, dx \\ &= \frac{\gamma_0}{\ln(2)} \widehat{E}\left(\ln(1+\gamma); \gamma_\circ\right) \end{aligned} \tag{27}$$

By using relation given below from [14]:

$$\ln(1+\gamma) = \int_0^{\infty} \left(\frac{1 - e^{-\gamma z}}{z}\right) e^{-z} dz \tag{28}$$

By substituting the value of $\ln(1+\gamma)$ form Equation (28) into Equation (27), we get:

$$C_{\mathrm{OPRA}} = \frac{\gamma_0}{\ln(2)} \int_0^{\infty} \frac{\left[1 - \hat{E}\left[e^{-xz};\gamma_\circ\right]\right]\ e^{-z}}{z}\, dz \tag{29}$$

Also, we define:

$$\begin{aligned} \hat{E}\left[e^{-xz};\gamma_0\right] &= \int_0^{\infty} e^{-xz} f_\gamma\left(\gamma_\circ(1+x)\right)\, dx \\ I_3 &= \int_0^{\infty} e^{-xz} f_\gamma\left(\gamma_\circ(1+x)\right)\, dx \end{aligned} \tag{30}$$

By putting the $\gamma_\circ(1+x) = g$ in Equation (30) and after some mathematical manipulation, the integral I_3 can be expressed as:

$$I_3 = \frac{e^z}{\gamma_0} \int_{\gamma_0}^{\infty} e^{-\frac{zg}{\gamma_0}} f_\gamma(g)\, dg = \frac{e^z}{\gamma_0} \hat{M}\left(\frac{z}{\gamma_0}, \gamma_0\right) \tag{31}$$

where $\hat{M}\left(\frac{z}{\gamma_0}, \gamma_0\right)$ is the MMGF. By putting value of I_3 from Equation (31) to the Equation (29), we get:

$$C_{\mathrm{OPRA}} = \frac{\gamma_0}{\ln(2)} \left[\int_0^{\infty} \frac{e^{-z}}{z} dz - \frac{1}{\gamma_0} \int_0^{\infty} \frac{\hat{M}\left(\frac{z}{\gamma_0}, \gamma_0\right)}{z} dz\right] \tag{32}$$

For evaluation of C_{OPRA}, in Equation (32), the first integral and second integral are required to evaluate, which can be obtained numerically by standard software like Maple and Mathematica. To obtain the optimal cut-off SNR $\gamma_\circ$ in Equation (32), we need to solve the Equation (25) by using standard techniques like as discussed in [5, 8, 12]. Here, we are presenting MMGF based approach for optimization of cut-off SNR $\gamma_\circ$. By rearranging the Equation (25), we get:

$$\frac{1}{\gamma_0} \int_{\gamma_0}^{\infty} f_\gamma(\gamma) d\gamma - \int_{\gamma_0}^{\infty} \frac{1}{\gamma_0} f_\gamma(\gamma) d\gamma = 1 \tag{33}$$

Also, we define:

$$I_4 = \frac{1}{\gamma_\circ} \int_{\gamma_0}^{\infty} f_\gamma(\gamma) d\gamma \tag{34}$$

and

$$I_5 = \int_{\gamma_0}^{\infty} \frac{f_\gamma(\gamma)}{\gamma} d\gamma \tag{35}$$

By substituting $s = 0$ and $a = \gamma_\circ$ in Equation (7), we get:

$$\hat{M}(0, \gamma_\circ) = \int_{\gamma_0}^{\infty} f_\gamma(\gamma) d\gamma \tag{36}$$

From Equation (34) and Equation (36), I_4 can be expressed as:

$$I_4 = \frac{\hat{M}(0, \gamma_\circ)}{\gamma_\circ} \tag{37}$$

By replacing $\frac{1}{\gamma} = \int_0^\infty e^{-\gamma s} ds$ in the Equation (35) and by changing the order of integration, we get:

$$I_5 = \int_0^\infty \left(\int_{\gamma_0}^\infty e^{-\gamma s} f_\gamma(\gamma) d\gamma \right) ds = \int_0^\infty \hat{M}(s, \gamma_0)\, ds \tag{38}$$

By substituting I_4 and I_5 in Equation (31), we get:

$$\frac{\hat{M}(0, \gamma_\circ)}{\gamma_\circ} - \int_0^\infty \hat{M}(s, \gamma_\circ)\, ds = 1 \tag{39}$$

where $\hat{M}(s, \gamma_0)$ is the MMGF of γ_0. From Equation (38) and Equation (12), the integral I_5 is evaluated as:

$$I_5 = \frac{A}{D} \sum_{k=0}^{\infty} \frac{\Gamma(k+m)\Gamma(Mm)}{\Gamma(m)\Gamma(k+Mm)} \frac{(C)^k}{k!}\, I_6 \tag{40}$$

where

$$I_6 = \int_0^\infty \frac{\Gamma(k + mM, \gamma_\circ(B + s))}{(B + s)^{(k+mM)}}\, ds \tag{41}$$

By substituting $B+s = t$ in the Equation (41) and after simplification, we get:

$$I_6 = \int_B^\infty \frac{\Gamma(k + mM, t)}{(t)^{(k+mM)}}\, dt \tag{42}$$

By using [23 Equation (8.4.16.2)], the Equation (42), can be expressed as:

$$I_6 = \int_B^\infty (t)^{-(k+mM)}\, G\,{}^{2\ 0}_{1\ 2}\left[\gamma_\circ t \,\middle|\, \begin{matrix} 1 \\ 0\quad 0 \end{matrix}\right] dt \tag{43}$$

and from [23 Equation (2.24.2.3)], the Equation (43) can be expressed as:

$$I_6 = (B)^{1-(k+mM)} G\,{}^{3\ 0}_{2\ 3}\left[B\gamma_\circ \,\middle|\, \begin{matrix} 1 & & k+mM \\ (k+mM)-1 & 0 & (k+mM) \end{matrix}\right] \tag{44}$$

By putting the result of I_6 from the Equation (44) in to Equation (40), we get:

$$I_5 = \frac{A}{D}\sum_{k=0}^{\infty}\frac{\Gamma(k+m)\Gamma(Mm)}{\Gamma(m)\Gamma(k+Mm)}\frac{(C)^k}{k!} \frac{G\,{}^{3\ 0}_{2\ 3}\left[B\gamma_\circ \,\middle|\, \begin{matrix} 1 & & k+mM \\ (k+mM)-1 & 0 & (k+mM) \end{matrix}\right]}{(B)^{(k+mM)-1}} \tag{45}$$

From Equation (12), integral I_4 can be expressed as

$$I_4 = \frac{\hat{M}(0,\gamma_\circ)}{\gamma_\circ} = \frac{A}{\gamma_\circ D}\sum_{k=0}^{\infty}\frac{\Gamma(k+m)\Gamma(Mm)}{\Gamma(m)\Gamma(k+Mm)}\frac{(C)^k}{k!}\frac{\Gamma(k+mM,\gamma_\circ)}{(B)^{(k+mM)}} \tag{46}$$

By substituting results of the Equations (45) and (46) in the Equation (39)

$$\left[\left(\frac{A}{\gamma_\circ D}\sum_{k=0}^{\infty}\frac{\Gamma(k+m)\Gamma(Mm)}{\Gamma(m)\Gamma(k+Mm)}\frac{(C)^k}{k!}\frac{\Gamma(k+mM,\gamma_\circ)}{(B)^{(k+mM)}}\right) - \left(\frac{A}{D}\sum_{k=0}^{\infty}\frac{\Gamma(k+m)\Gamma(Mm)}{\Gamma(m)\Gamma(k+Mm)}\frac{(C)^k}{k!} \times \frac{G\,{}^{3\ 0}_{2\ 3}\left[B\gamma_\circ \,\middle|\, \begin{matrix} 1 & & k+mM \\ (k+mM)-1 & 0 & (k+mM) \end{matrix}\right]}{(B)^{(k+mM)-1}}\right)\right] = 1 \tag{47}$$

Although, the optimal cut-off SNR $\gamma_\circ$ cannot be obtained in closed-form by Equation (47), in order to get optimal cut-off SNR, $\gamma_\circ$, the numerical evaluation is performed using standard software like Mathematica or Maple.

4.3. Channel Inversion With Fixed Rate

The channel capacity for channel inversion with fixed rate (C_{CIFR}) requires that the transmitter exploits the channel state information such that the constant SNR is maintained at receiver. In this method, fixed transmission rate is used since the channel after fading inversion appears. The channel capacity with fixed channel inversion rate can be expressed as [8]:

$$C_{\text{CIFR}} = \log_2 \left(1 + \frac{1}{\int_0^\infty \frac{f_\gamma(\gamma)}{\gamma} d\gamma} \right) \tag{48}$$

The Equation (48) can be expressed in the term of MGF as shown below:

$$I_7 = \int_0^\infty \frac{f_\gamma(\gamma)}{\gamma} d\gamma \tag{49}$$

By replacing $\frac{1}{\gamma} = \int_0^\infty e^{-\gamma s} ds$ in the Equation (49), we get:

$$I_7 = \int_0^\infty f_\gamma(\gamma) \left(\int_0^\infty e^{-\gamma s} ds \right) d\gamma \tag{50}$$

By changing order of the integration in Equation (50), we get:

$$I_7 = \int_0^\infty \left(\int_0^\infty f_\gamma(\gamma) e^{-\gamma s} d\gamma \right) ds$$

Now, we have

$$I_7 = \int_0^\infty M(s) ds \tag{51}$$

By putting the value of I_7 from the Equation (51) in Equation (48), we get:

$$C_{\text{CIFR}} = \log_2 \left(1 + \frac{1}{\int_0^\infty M(s)\, ds} \right) \tag{52}$$

By putting the value of $M(s)$, from Equation (15) in Equation (51), we get:

$$I_7 = \int_0^\infty \left(1+\frac{\bar{\gamma}_t(1-\rho+M\rho)\,s}{m}\right)^{-m}\left(1+\frac{\bar{\gamma}_t(1-\rho)\,s}{m}\right)^{-m(M-1)} ds \quad (53)$$

By using [22 Equation (3.259.3)], the integral I_7 in the Equation (53) can be expressed as:

$$I_7 = \frac{m\,B(1,mM-1)}{(1+\rho(M-1))\bar{\gamma}_t}\,{}_2F_1\left(m(M-1),1;\,mM;\,\frac{M\rho}{1+\rho(M-1)}\right) \quad (54)$$

where $B(\cdot)$ is beta function [22, Equation (8.384.1)]. By putting the result of Equation (54) into the Equation (52), we get:

$$C_{\mathrm{CIFR}} = \log_2\left(1+\frac{(1+\rho(M-1))\bar{\gamma}_t}{m\,B(1,mM-1)\,{}_2F_1\left(m(M-1),1;mM;\frac{M\rho}{1+\rho(M-1)}\right)}\right) \quad (55)$$

The above expression evaluates the accurate value of channel capacity for channel inversion with fixed rate scheme for arbitrary value of the fading parameter (m).

4.4. Truncated Channel Inversion

The CIFR suffers from a large capacity penalty relative to other techniques. The truncated CIFR is a better approach than that of CIFR, where channel fading is inverted above a cut-off SNR (γ_0). The channel capacity for a truncated CIFR is defined as [8].

$$C_{\mathrm{TCIFR}} = \log_2\left(1+\frac{1}{\int_{\gamma_0}^{\infty}\frac{f_\gamma(\gamma)}{\gamma}d\gamma}\right)\{1-P_{\mathrm{out}}(\gamma_\circ)\} \quad (56)$$

In Equation (54), the integral $\int_{\gamma_0}^{\infty}\frac{f_\gamma(\gamma)}{\gamma}d\gamma$ is similar with the integral I_5 in Equation (35) and it can be written in terms of MMGF as given in Equation (36). The outage probability $P_{\mathrm{out}}(\gamma_\circ)$ expressed in the Equation (26) can be written as:

$$P_{\mathrm{out}}(\gamma_\circ) = 1-\int_{\gamma_\circ}^{\infty} f_\gamma(\gamma)\,d\gamma \quad (57)$$

By using Equation (37), the Equation (57) can be expressed as:

$$P_{\text{out}}(\gamma_\circ) = 1 - \hat{M}(0, \gamma_\circ) \tag{58}$$

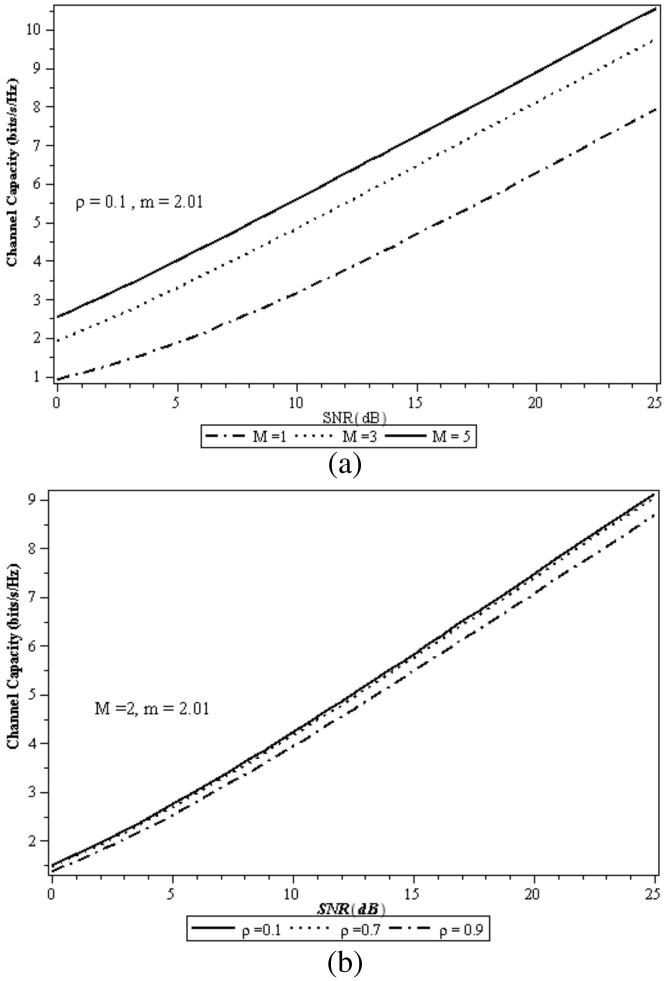

Figure 1. Channel capacity with optimal rate adaptation (C_{ORA}) versus SNR for various (a) diversity receivers and (b) correlation coefficients.

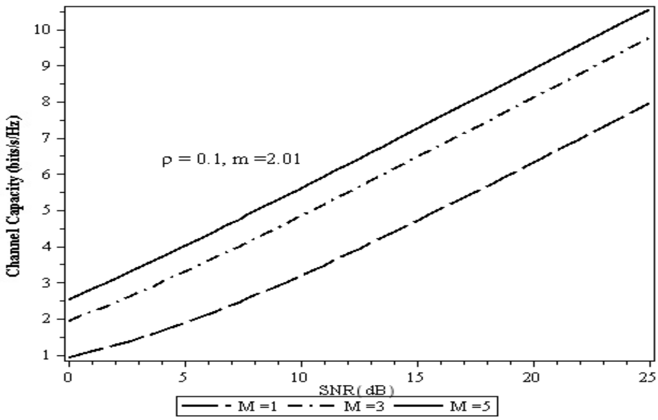

(a)

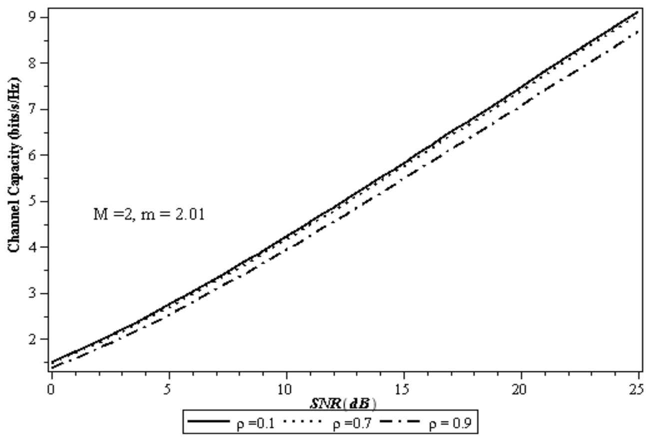

(b)

Figure 2. Channel capacity for optimal rate adaptation (C_{OPRA}) versus SNR for various (a) diversity receivers and (b) correlation coefficient.

By putting $a = \gamma_\circ$ and $s = 0$ in Equation (12), $P_{\mathrm{out}}(\gamma_\circ)$ can be expressed as:

$$P_{\mathrm{out}}(\gamma_\circ) = 1 - \frac{A}{D} \sum_{k=0}^{\infty} \frac{\Gamma(k+m)\Gamma(Mm)}{\Gamma(m)\Gamma(k+Mm)} \frac{(C)^k}{k!} \frac{\Gamma(k+mM, \gamma_\circ B)}{(B)^{(k+mM)}} \quad (59)$$

$$C_{\mathrm{TCIFR}} = \log_2 \left(1 + \frac{1}{\int\limits_0^{\infty} \hat{M}(s, \gamma_0)\, ds} \right) \left\{ \hat{M}(0, \gamma_\circ) \right\} \quad (60)$$

By substituting result of I_5 from the Equation (45) and P_{out}, in Equation (60), we get:

$$C_{\text{TCIFR}} = \log_2\left(1+\frac{1}{\left(\frac{\frac{A}{D}\sum_{k=0}^{\infty}\frac{\Gamma(k+m)\Gamma(Mm)}{\Gamma(m)\Gamma(k+Mm)}\frac{(C)^k}{k!}G^{3\ \ 0}_{2\ \ 3}\left[B\gamma_\circ\Big|\begin{matrix} & 1 & k+mM\\ (k+mM)-1 & 0 & (k+mM)\end{matrix}\right]}{(B)^{(k+mM)-1}}\right)}\right)\left\{\hat{M}(0,\gamma_\circ)\right\} \tag{61}$$

By using the Equation (61), the channel capacity for the truncated CIFR scheme can be evaluated easily for arbitrary value of the fading parameter.

5. RESULTS AND DISCUSSION

In this section, we have presented some numerical results for the channel capacity with MRC diversity at receiver over the correlated Nakagami-m fading channel. Fig. 1 shows the channel capacity with optimal rate adaptation (C_{ORA}) as a function of the SNR for various diversity receivers as well as correlation coefficients. As the number of diversity receiver increases, the C_{ORA} improves significantly as shown in Fig. 1(a). Fig. 1(b) depicts the effect of correlation coefficient on the channel capacity with optimal rate adaptation (C_{ORA}) as a function of SNR. As the correlation coefficient increases, the C_{ORA} decreases as shown in Fig. 1(b). Fig. 2 shows the channel capacity for optimal power and rate adaptation (C_{OPRA}) versus SNR for various diversity receivers and correlation coefficients. As the number of diversity receivers increases, the C_{OPRA} improves as shown in the Fig. 2(a). Fig. 2(b) shows the channel capacity for (C_{OPRA}) versus SNR for several values of correlation coefficient as shown in Fig. 2(b). Fig. 3 shows the graph between the channel inversion with fixed rate (CIFR) and SNR for various diversity receivers as well correlation coefficients. The CIFR improves with the increasing of diversity receiver as shown in Fig. 3(a). Fig. 3(b) shows the channel inversion with fixed rate (CIFR) versus SNR for several correlation coefficients. As it increases, the CIFR decreases but the decrement is more in comparison to that of the Fig. 1(b) and Fig. 2(b). Fig. 4 shows the channel capacity with truncated channel inversion (C_{TCIFR}) versus cut-off SNR (γ_0) for various values of the SNR. From Fig. 4, it is seen that as the SNR increase, the cut-off rate (γ_0) also increases. Fig. 5 shows the channel capacity with truncated channel inversion (C_{TCIFR}) versus cut-off rate (γ_0) for various MRC diversities. As the MRC diversity increases, the cut-off rate (γ_0) increases significantly as shown in

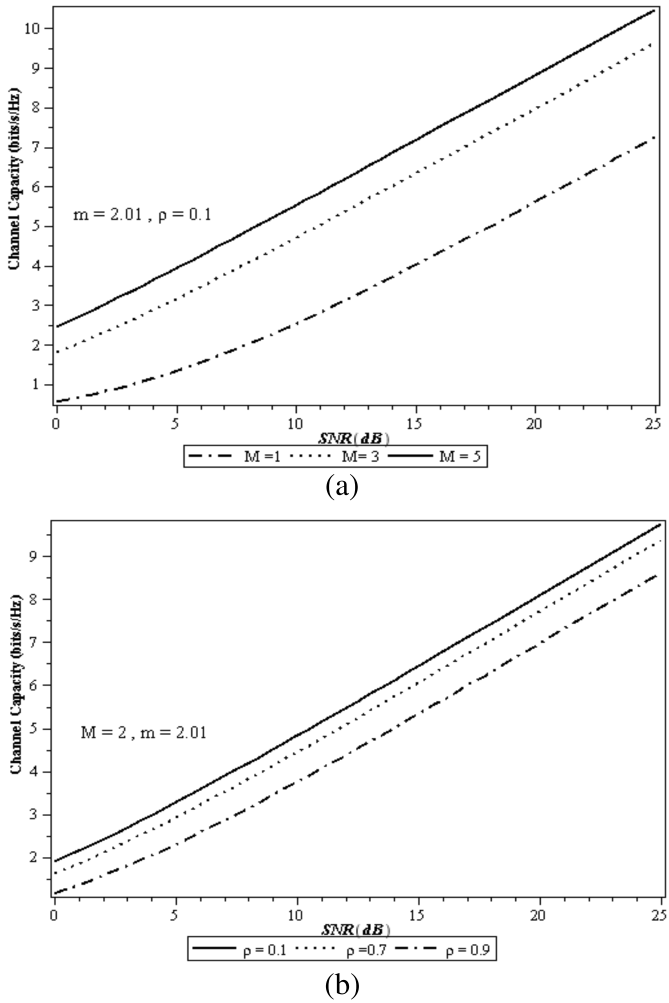

Figure 3. Channel inversion with fixed rate (CIFR) versus SNR for various (a) diversity receivers and (b) correlation coefficients.

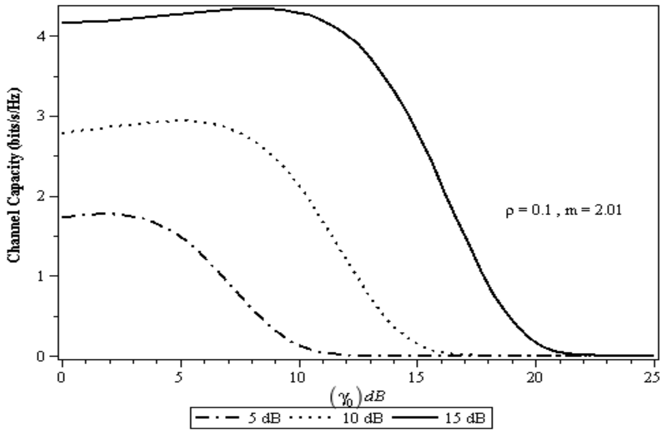

Figure 4. Channel capacity with truncated channel inversion (C_{TCIFR}) versus cut-off SNR (γ_0) for various values of SNR.

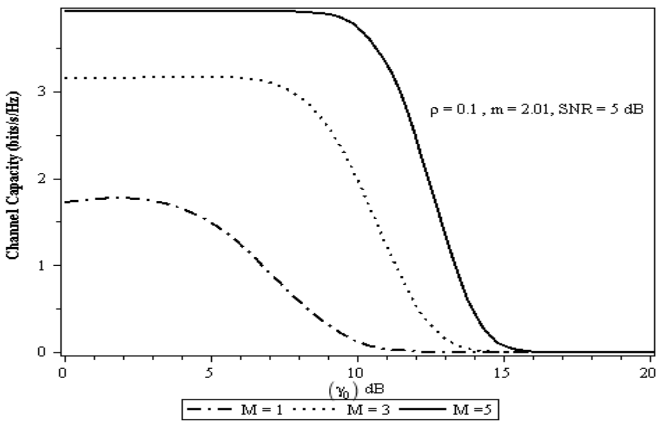

Figure 5. Channel capacity with truncated channel inversion (C_{TCIFR}) versus cut-off SNR (γ_0) for different MRC diversity.

Fig. 5. Fig. 6 depicts the channel capacity with truncated channel inversion (C_{TCIFR}) versus cut-off SNR (γ_0) for the various values of the correlation coefficient. As the correlation coefficient increases, the cut-off rate decreases slowly.

Figures 7 to 10 show the comparison of channel capacity under various adaptive condition with the reported literature [12] for correlated Rayleigh fading channel ($m = 1$). The result of the proposed method is similar with that of [12]. In the Fig. 7, the characteristic of the channel capacity for optimal rate adaptation with correlation coefficients of the proposed method has been compared with [12] by considering the Rayleigh fading channel ($m = 1$). The results of the proposed method are comparable with that of the [12]. In Fig. 8 shows the comparison of the characteristics of channel capacity for optimal simultaneous power and rate adaptation with SNR for

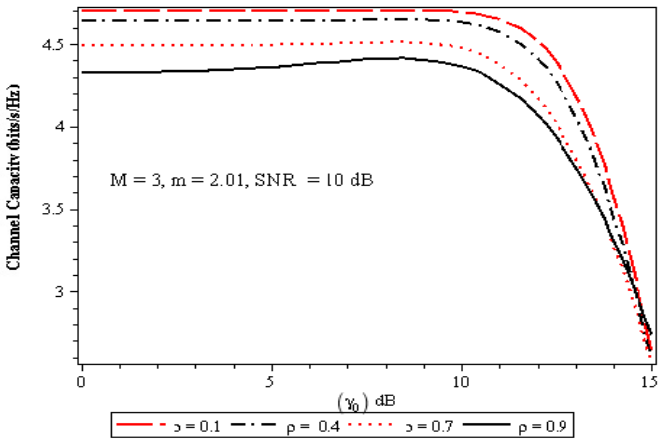

Figure 6. Channel capacity with truncated channel inversion (C_{TCIFR}) versus cut off SNR (γ_0) for the various value of correlation coefficient.

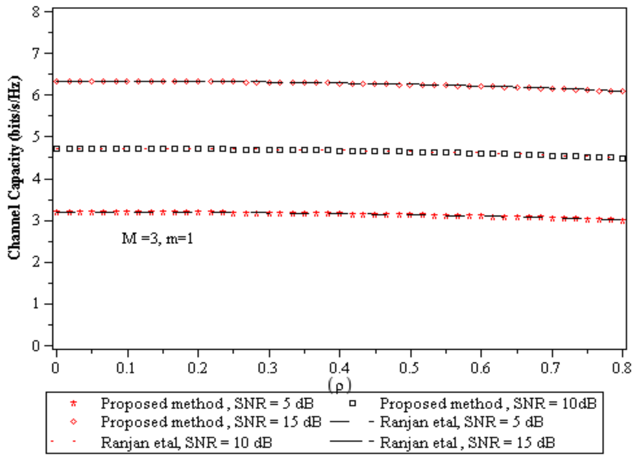

Figure 7. Comparison of the capacity with [12] for optimal rate adaptation (C_{ORA}) versus correlation coefficient for diversity $M = 3$ for different values of SNR.

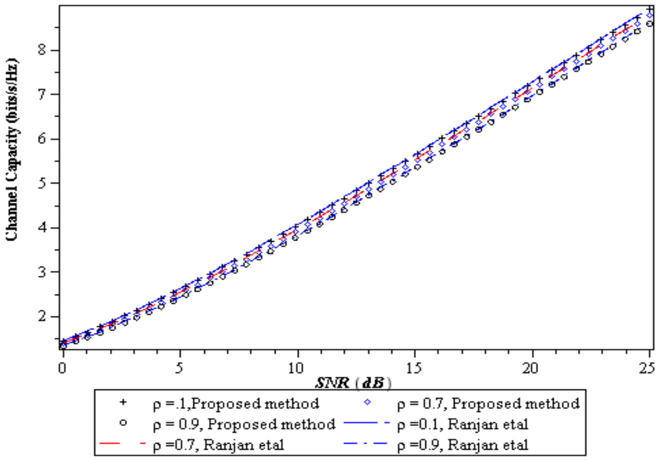

Figure 8. Comparison of the channel capacity with [12] for optimal rate adaptation (C_{OPRA}) versus SNR for the several values of correlation coefficient.

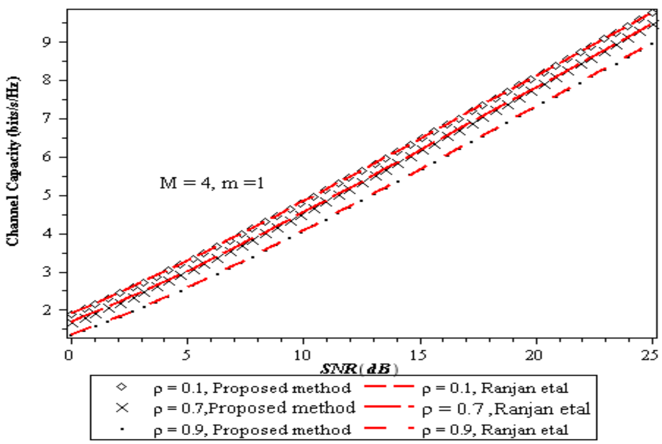

Figure 9. Comparison of the channel inversion with [12] for fixed rate (CIFR) versus SNR for various correlation coefficients.

various correlation coefficients of the proposed method with [12] by considering the Rayleigh fading channel ($m = 1$). The results of the proposed method are comparable with that of the [12]. Fig. 9 depicts the comparison of the characteristics of channel capacity of channel inversion with fixed rate with SNR for various correlation coefficients of the proposed method with [12] by considering the Rayleigh fading

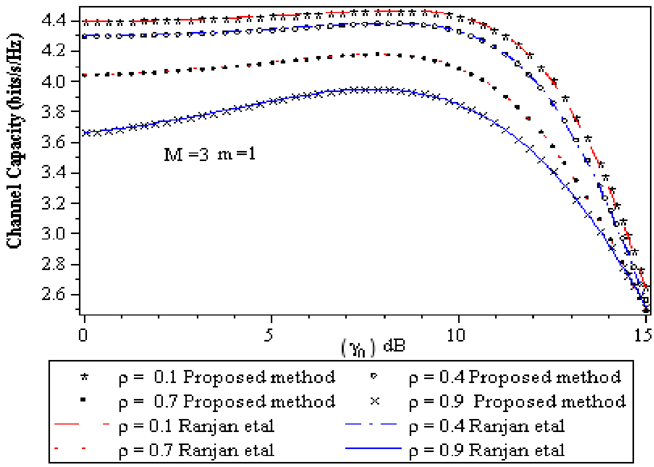

Figure 10. Comparison of the channel capacity with [12] for truncated channel inversion (C_{TCIFR}) versus cut off SNR (γ_0) for various correlation coefficients.

channel ($m = 1$). The results of the proposed method are comparable with that of the [12].

In Fig. 10, we have compared the characteristics of channel capacity of channel inversion with truncated channel (C_{TCIFR}) versus cut-off SNR (γ_0) for various correlation coefficients of the proposed method with [12] by considering the Rayleigh fading channel ($m = 1$). The results of the proposed method are comparable with that of the [12].

6. CONCLUSIONS

In this paper, we have investigated the marginal MGF for correlated Nakagami-m fading channel with MRC diversity and obtained marginal MGF is used to evaluate the channel capacity under different adaptation policies. A novel mathematical expression for the computation of channel capacity under various adaptive schemes is derived which is valid for arbitrary value of the fading parameters m. We have also analyzed the effect of correlation on the channel capacity. Due to their simple forms, these results offer a useful analytical tool for the accurate performance evaluation of the various systems of practical interest.

ACKNOWLEDGMENT

The authors are sincerely thankful to the unanimous reviewers for their critical comments and suggestions to improve the quality of the manuscript.

REFERENCES

1. Simon, M. K. and M.-S. Alouini, *Digital Communication over Fading Channels*, 2nd Edition, Wiley, New York, 2005.
2. Proakis, J. G., *Digital Communications*, 4th Edition, McGraw-Hill Series, SDLS, 2001.
3. Varzakas, P. and G. S. Tombras, "Spectral efficiency of a cellular MC/DS-CDMA system in Rayleigh fading," *International Journal of Communication Systems*, Vol. 18, No. 8, 795–801, Oct. 2005.
4. Varzakas, P. and G. S. Tombras, "Spectral efficiency of a single cell multi-carrier DS-CDMA system in Rayleigh fading," *Journal of the Franklin Institute-Engineering and Applied Mathematics*, Vol. 343, 295–300, 2006.
5. Goldsmith, A. and P. Varaiya, "Capacity of fading channels with channel side information," *IEEE Trans. Inform. Theory*, Vol. 43, No. 6, 1896–1992, Nov. 1997.
6. Lee, W. C. Y., "Estimate of channel capacity in Rayleigh fading environment," *IEEE Trans. on Veh. Technol.*, Vol. 93, No. 39, 187–189, Aug. 1990.
7. Gunther, C. G., "Comment on estimate of channel capacity in Rayleigh fading environment," *IEEE Trans. on Veh. Technol.*, Vol. 45, No. 2, 401–403, May 1996.
8. Alouini, M. S. and A. J. Goldsmith, "Capacity of Rayleigh fading channels under different adaptive transmission and diversity-combining techniques," *IEEE Trans. on Veh. Technol.*, Vol. 48, No. 4, 1165–1181, Jul. 1999.
9. Karagiannidis, G. K., N. C. Sagias, and G. S. Tombras, "New results for the Shannon channel capacity generalized fading channels," *IEEE Commun. Lett.*, Vol. 9, No. 2, 97–99, Feb. 2005.
10. Khatalin, S. and J. P. Fonseka, "On the channel capacity in Rician and Hoyt fading environment with MRC diversity," *IEEE Trans. on Veh. Technol.*, Vol. 55, No. 1, 137–141, Jan. 2006.
11. Khatalin, S. and J. P. Fonseka, "Capacity of correlated Nakagami-m fading channels with diversity combining techniques," *IEEE Trans. on Veh. Technol.*, Vol. 55, No. 1, 142–150, Jan. 2006.

12. Mallik, R. K., M. Z. Win, J. W. Shao, M.-S. Alouini, and A. J. Goldsmith, "Channel capacity of adaptive transmission with maximal ratio combining in correlated Rayleigh fading," *IEEE Trans. Wireless Commun.*, Vol. 3, No. 4, 1124–1133, Jul. 2004.
13. Zhang, Q. T. and D. P. Liu, "Simple capacity formulas for correlated SIMO Nakagami channels," *Proc. IEEE Veh. Technol. Conf.*, Vol. 1, 554–556, Apr. 2003.
14. Hamdi, K. A., "Capacity of MRC on correlated Rician fading channels," *IEEE Trans. on Commun.*, Vol. 56, No. 5, 708–711, May 2008.
15. Palat, R. C., A. Annamalai, and J. H. Reed, "An efficient method for evaluating information outage probability and ergodic capacity of OSTBC system," *IEEE Commun. Lett.*, Vol. 12, No. 3, 191–193, Mar. 2008.
16. Renzo, M. D., F. Graziosi, and F. Santucci, "Channel capacity over generalized fading channels: A novel MGF-based approach for performance analysis and design of wireless communication systems," *IEEE Trans. on Veh. Technol.*, Vol. 59, No. 1, 127–149, Jan. 2010.
17. Park, S. Y., D. J. Loveand, and D. H. Kim, "Capacity limits of multi-antenna multicasting under correlated fading channels," *IEEE Trans. on Commun.*, Vol. 58, No. 7, 2002–2013, Jul. 2010.
18. Brennan, D. G., "Linear diversity combining techniques," *Proc. IRE*, Vol. 47, No. 6, 1075–1102, Jun. 1959.
19. Dwivedi, V. K. and G. Singh, "A novel moment generating function based performance analysis over correlated Nakagami-m fading," *Journal of Computational Electronics*, Vol. 10, No. 4, 373–381, Dec. 2011.
20. Dwivedi, V. K. and G. Singh, "Error-rate analysis of OFDM communication system in correlated Nakagami-m fading channel using maximal ratio combining diversity," *International Journal of Microwave and Wireless Technologies*, Vol. 3, No. 6, 717–726, Dec. 2011.
21. Aalo, V. A., "Performance of maximal-ratio diversity systems in a correlated Nakagami-fading environment," *IEEE Trans. on Commun.*, Vol. 43, No. 8, 2360–2369, Aug. 1995.
22. Gradshteyn, I. S. and I. M. Ryzhik, *Table of Integrals, Series, and Products*, 7th Edition, Academic, New York, 2007.
23. Prudnikov, A. P., Y. A. Brychkov, and O. I. Marichev, *Integrals and Series: More Special functions*, Vol. 3, Gordon and Breach Science, 1990.

24. Theofilakos, P., A. G. Kanatasand, and G. P. Efthymoglou, "Performance of generalized selection combining receivers in K-fading channels," *IEEE Commun. Lett.*, Vol. 12, No. 11, 816–818, Nov. 2008.
25. Abramowitz, M. and I. A. Stegun, *Handbook of Mathematical Functions: With Formulas, Graphs, and Mathematical Tables*, Dover Publications, New York, 1970.